https://www.scirp.org/journal/jbise

J. Biomedical Science and Engineering,
2023, Vol. 16, (No. 5), pp: 65-79

Morphogenesis of Floating Bone Segments: A Legacy of Serial Tensile Cross-Strut Microdamage in Trabecular Disconnection "Crumple Zones"?

Patricia A. Shore[1], Roger C. Shore[2], Jean E. Aaron[1]

[1]School of Biomedical Sciences, University of Leeds, Leeds, UK; [2]Division of Oral Biology, Leeds School of Dentistry, University of Leeds, Leeds, UK

Correspondence to: Jean E. Aaron, j.e.aaron@leeds.ac.uk

Keywords: Skeletal Fragility, Microdamage, Tensile Trabecular Disconnection, Floating Segments and Bony Spheroids, Substructural Crumple Zones, SEM and EDS Microanalysis

Received: April 26, 2023 **Accepted:** May 28, 2023 **Published:** May 31, 2023

ABSTRACT

Trabecular bone disconnection "hotspots" of real termini (ReTm) previously mapped as loci of weakness in the female aging spine and hip may be a source of free-floating cancellous segments found in the medullary space using a bespoke, thick slice histological method for identifying ReTm. A factor in their origin is apparently microdamage proliferation (differentiated by *en bloc* silver staining) with occasional callus moderation. Validation of similar "floating segments" (FS) in the ex-breeder rat suggested a pilot model for a potentially common phenomenon. Following marrow elution and density fractionation of the isolated floating segments from the whole proximal rat femora, scanning electron microscopy (SEM) and elemental microanalysis (EDS) was performed. The eluent contained numbers of vertically truncated, laterally branched floating segments (<1 mm) together with bony spheroids. ReTm were a defining feature, ranging from smoothly elliptical, to coarsely textured by exposed populations of substructural calcified microparticles (<1 μm). While EDS spectra of the ReTm stumps registered little trace element distinction, their matrix mineral density was significantly lower than elsewhere. It was concluded that floating bone segments are the microarchitectural consequence of destabilised ReTm hotspot domains primed by local microdamage. Their common format of serial trabecular projections from a truncated central axis combines i) *acute* severance of sequential tensile cross-struts, causing *chronic* compression overload of axial-struts, with ii) inadequate stabilising callus, facilitating ReTm stacking into predetermined, substructural "crumple zones" of force containment, spheroidal attrition and particulate dissociation. As a catabolic outcome of altered tensile and

hormonal influence, FS number may add a novel variable to cancellous bone kinetics particularly in women of relevance to fracture predisposition.

1. INTRODUCTION

Bone mass is a well-recognized determinant of fracture predisposition in the elderly such that those with minimum trauma fractures tend to have a low mean bone mass. However, some individuals with an apparently adequate bone mass nevertheless sustain atraumatic fractures, whereas others with a deficient bone mass do not. In explanation, reports continue to suggest that the strength of the aging skeleton is diminished by an intrinsic deterioration in the trabecular microarchitecture with special reference to trabecular disconnection which weakens bone disproportionate to the volume lost. Because the histomorphometry of this variable in thin sections can be misleading due to planar sectioning artefacts, we previously developed a direct method using undecalcified, thick slice (300 μm) histology [1] which more reliably identifies real trabecular disconnection termini (ReTm) [2] [3]. When applied to normal aging human spine and hip, where the cancellous bone framework is especially vulnerable to microdamage, it was observed that an increase in cross-strut severance contributes to skeletal failure in women (less so in men [4]). Moreover, ReTm mapping shows a marked tendency to accumulate in predictable ReTm "hotspot" domains, especially in relation to transverse axes of tensile stress [3, 5]. The evidence suggests that these loci of fragility may be the source of the bony islands occasionally observed in the marrow spaces as "floating segments" (FS). These relics of microanatomical attrition, surrounded by intact tissue and with intermittent signs of callus repair [6], seem unlikely artefacts of preparation. Moreover, ReTm are rare in youth, apart from a transitory appearance during the trabecular microarchitectural modulation that accompanies mammalian reproduction [7]. The latter is exacerbated in the ex-breeder laboratory rat, an animal supporting successive multiparous pregnancies at the end of which a decline in the trabecular number has been reported at several sites, relative to virgin controls [8].

With the objective of applying established techniques of density fractionation and microanalysis to an osteopenic model, the aim was to determine the process of floating segment morphogenesis in trabecular bone atrophy as a complementary addendum to our earlier report [5] mapping ReTm in thick slices of the aging female spine and hip.

2. MATERIALS AND METHODS

As a small-scale pilot demonstration of trabecular microdamaged disconnection in aging women, the mineralised matrix was examined in representative archival, cadaveric digits (donations in accordance with the Human Tissues Act). These were *en-bloc* stained (*i.e.*, in bulk) in silver nitrate by an established procedure [9] using the von Kossa silver stain prior to embedding and longitudinal planar sectioning (75 μm) on a heavy-duty microtome (Reichert-Jung, Heidelberg); this process distinguished *in situ* stained microdamage from unstained preparation artefact as a factor in human skeletal attrition.

An extensive literature relates to the rat as a skeletal model in primary stage investigations (e.g., osteopenia after ovariectomy). In that tradition, the remains of 7 adult ex-breeder Wistar females became available at the conclusion of an approved regimen (optimum temperature, light and ad libitum food) of reproduction which had commenced at aged three months and continued for 3 successive breeding cycles of gestation, lactation and weaning, with interludes of one week between pregnancies, and with nulliparous controls (see [8] for details). Analysis comprised thin histological sections, thick slices and SEM and EDS of density fractionated isolates.

Left femora stripped of attached soft tissue were used to provide histological evidence of trabecular disconnection (ReTm) into floating segments *in situ*. They were embedded intact in methylmethacrylate preparatory to undecalcified longitudinal thick slicing (300 μm) of the whole femora using a Microslice 2 (Metals Research Ltd., Cambridge). Superficial staining of upper and lower surfaces of the thick slices with the von Kossa silver stain separated ReTm (unstained) from stained planar artefacts [1, 3].

Right femora were selected as the source of isolated floating segments as discrete objects and were bisected mid-diaphysis. The marrow was eluted by immersion in 0.75M NaOH at 55˚C for 30 min, 1 hr, 2 hr and 1 week respectively ([9] using the protocol established by Odgaard *et al.*, Bone, 1994). It was found that after 30 min there was no further increase in the number of "floating segments". The dense fraction was separated from the marrow cell debris by centrifugation and the presence of discrete isolated bone segments was confirmed in polarised light by their lamellar birefringence and osteocyte networks. Their topology was determined by scanning electron microscopy (SEM) and their mineral composition by elemental microanalysis (EDS, including line-scan spectra). The EDS data were compared between disconnected lateral struts (*i.e.*, ReTm) and interconnected axial junctions (*i.e.*, trabecular nodes TbN).

3. RESULTS

Floating segments of cancellous bone, previously suggested in the aging female skeleton and repeated in a multiparous animal (Aaron *et al.* [5] *fig 10d-f*], were substantiated in the ex-breeder rats as follows. The morphometric objects were defined by multiple ReTm, consistent with microdamage proliferation generated in response to a combination of reproductive hormones and altered mechanical stress.

1) *Floating segments, resorption and microdamage in situ and in isolation.* The general appearance of sites of microdamage in *en bloc* silver-stained material from elderly subjects was shown by back-scattered SEM examination of thick optical sections as matrix leakiness, stained microfissures and wider microcracks (**Figure 1(a)**, **Figure 1(b)**). Their propagation from minor faults was demonstrated in back-scattered SEM images of thick slices where sequential cross-strut microdamage apparently caused the severance of tracts of bony islands (**Figures 1(c)-(h)**). Traces of callus repair were confined to axial-struts (**Figure 2(a)**, **Figure 2(b)**), while bridging of a different fibrous nature (**Figure 2(c)**, **Figure 2(d)**) was an occasional polarised response to cross-strut division.

Against this background of age-related matrix microdamage, floating segments supported by marrow tissue were observed *in situ* as discrete entities using light microscopy of thick slices (**Figure 3(a)**). Unlike silver-stained, planar sectioning artefacts, real disconnected segments were colourless islands of bone defined by their unstained ReTm. Similar complex objects were recurrent in the density-fractionated eluent (**Figure 3(b)**, **Figure 3(c)**). The largest floating segments (about a millimetre in size) were convoluted in shape, typically consisting of a truncated axis from which projected serial, lateral ReTm stumps (**Figure 3(d)**), which were variously irregular, smooth or textured (**Figure 3(e)**). Similar, smaller objects (**Figure 3(f)**) were rounded into bony spheroids (50 - 100 μm diameter) with a differentially eroded substructure of calcified microspheres (<1 μm) [10] variably deformed by compaction (**Figure 3(g)**, **Figure 3(h)**).

2) *Floating segments and elemental microanalysis.* EDS spectra of the isolated segments registered prominent peaks for calcium and phosphorous relative to carbon (**Table 1**). The spectra of ReTm indicated a significantly lower bone density as shown by a reduced Ca:C ratio than that of the interconnected junctional nodes and mid-central axis (**Figure 4**). At the same time, there was no inorganic distinction linking the material properties of the ReTm disconnection stumps to regional trace element "doping".

Application of elemental line-scan mode to the thick sections of human digit samples as their bone surface was traversed enabled the direct mapping of matrix elemental spectra for Ca, C, N, Si, Mg and P in register with the corresponding topography. Although little consistent variation in regional trace element distribution was found (**Table 2**), a notable exception was Si peaks coincident with a site of parallel Sharpey's fibre insertions (**Figure 5**).

4. DISCUSSION

The floating segment question arose as an addendum to the earlier application of our "in house" method [3] pinpointing human trabecular disconnection as a pivotal histomorphometric variable of fragility and mapped at complex multiaxial fracture sites by Aaron *et al.* [5]. In that communication and illustrated by microCT [5, *Fig. 6d*] were parallel disconnected cross struts as serial ReTm stumps between prominent linear arrays of vertical trabeculae as a potential construct for the release of floating segments.

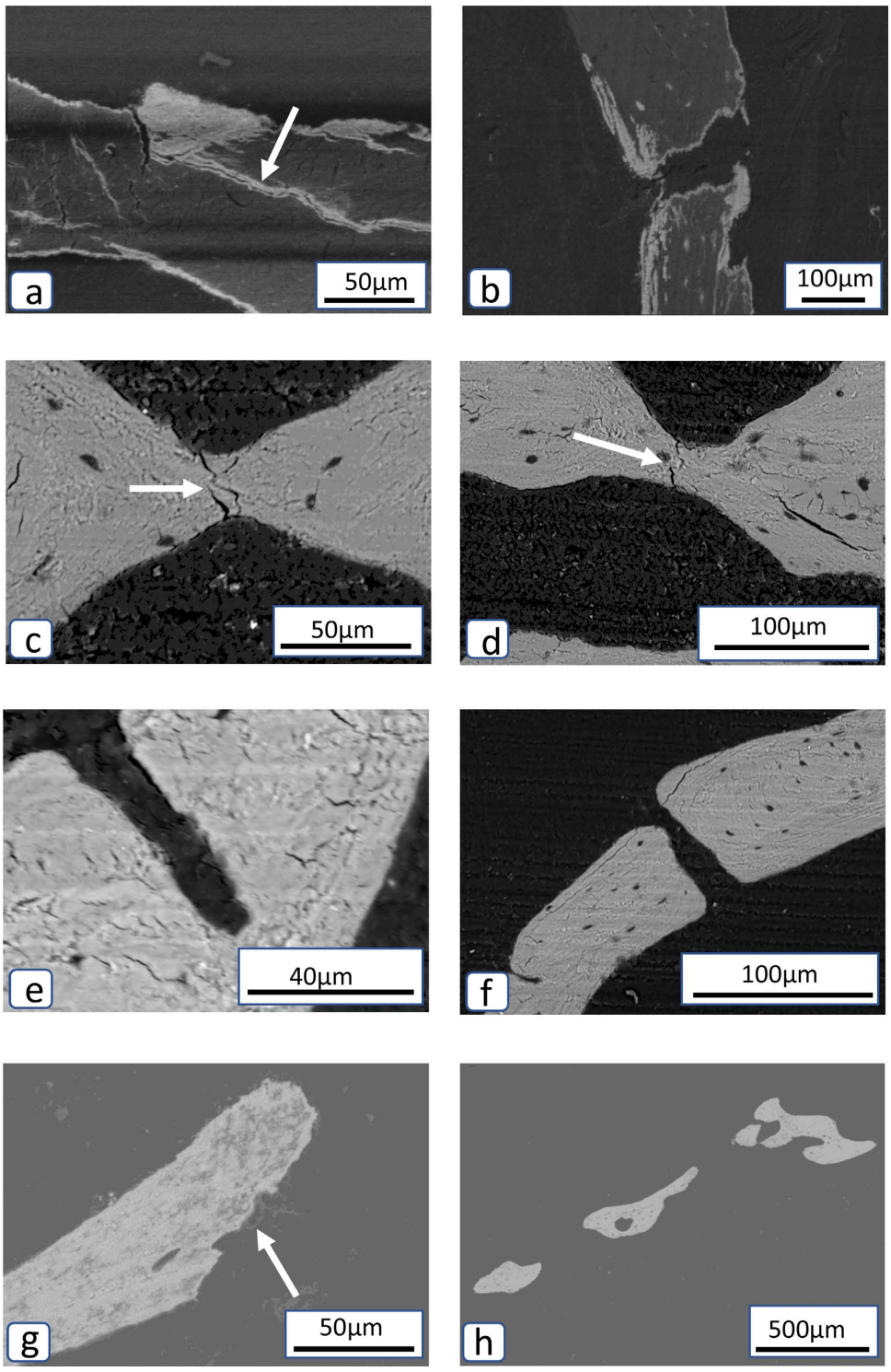

Figure 1. Microdamage and cross-strut disconnection, typical of elderly long bone. (a) Back-scattered SEM showing trabecular microfissures (arrowed) and (b) microcracks, bulk-stained with von Kossa silver stain. ((c), (d)) Back-scattered SEM showing mid-shaft trabecular microfissures (arrowed) in separate cross-strut locations, together with ((e), (f)) completion of trabecular severance with (g) a disconnection terminus (and signs of osteoclasis, arrowed), contributing to multiple floating segments (h). Plastic-embedded sections, 75 µm thick.

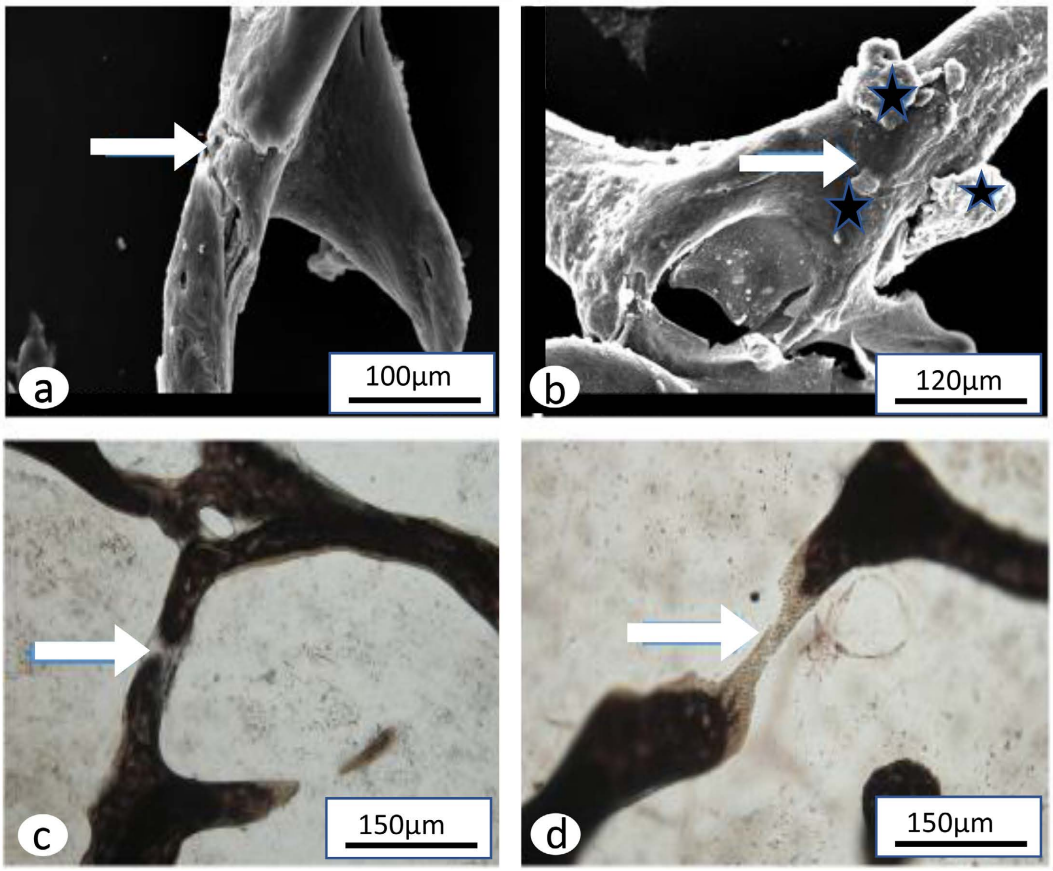

Figure 2. Microdamage and restitution. (a) Trabecular axial strut microcracks (arrowed), and (b) with microcallus repair (star); SEM, rodent long bone isolates. ((c), (d)) Trabecular cross-strut severance, bridged by uncalcified endosteal fibre bundles (arrowed); LM, plastic-embedded section.

Table 1. Comparison of the mineral topographic density of convoluted floating segments measured as the calcium:carbon ratio (Ca:C) by EDS microanalysis, showing the significantly lower matrix calcium content of the ReTm (stumps) relative to the main trabecular axis (mid-shaft) and intact junctional nodes.

Trabecular Ca:C Ratio		
	ReTm (Stumps)	Axis + Junctional nodes
Mean	0.67	2.60
S.D.	0.76	1.21
N	10	6
ReTm (Stumps) *v.* Axis + Junctional nodes		
	$p < 0.007$ (1 tail)	
	$P < 0.014$ (2 tail)	

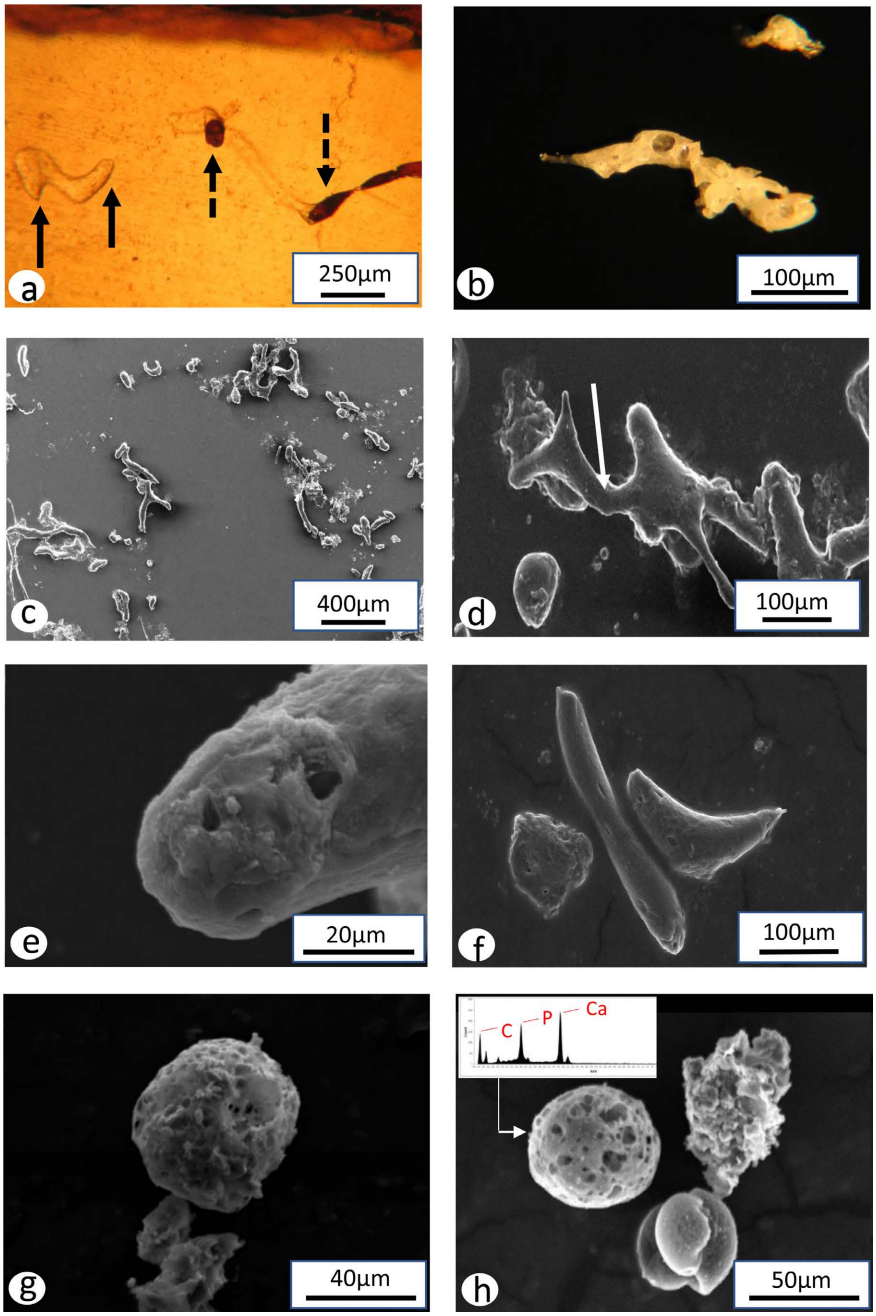

Figure 3. Floating segments (FS) in section and isolated from rodent long bone. (a) FS *in situ* within the marrow space, showing convoluted morphology and unstained ReTm (arrowed), contrasting with nearby stained artefactual termini (broken arrows); LM, plastic-embedded slice, 300 µm thick; (b) isolated FS showing resorption cavities and convoluted morphology by reflected LM. (c) FS isolates showing a complex and simple morphology in density-fractionated eluent, low power SEM; (d) large, convoluted FS with a main axial-strut (arrowed) and multiple lateral ReTm stumps, high power SEM. (e) FS isolate showing a rough, textured ReTm (stump) and (f) a trio of simple floating segments with smooth surfaces disrupted in part by exposed mineral substructure, SEM. ((g), (h)) Floating segments as bony spheroids showing lytic attrition and particulate disintegration, SEM; (inset shows corresponding EDS spectrum of C, P and Ca peaks typical of bone mineral).

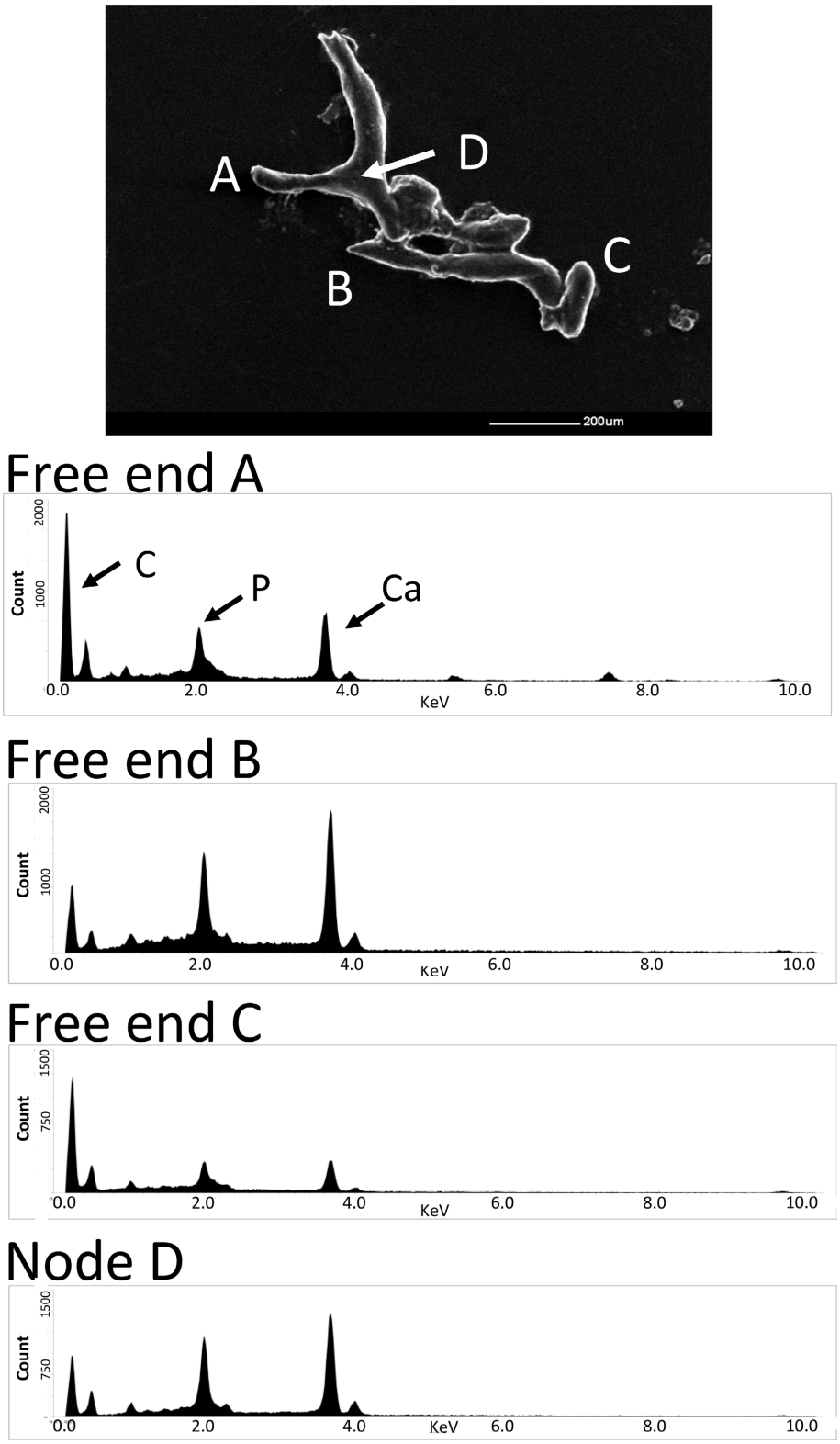

Figure 4. Convoluted FS showing a trabecular axis with lateral projections, interconnected junction (nodes) and ReTm (free ends); SEM. Comparison of EDS spectra for free ends A, B C, and node D. Peak heights for Ca, P and background organic matrix carbon show a lower bone mineral density (*i.e.*, greater C:Ca ratio) at rounded free ends than inner node.

Table 2. Elemental microanalysis (EDS) showing the composition in floating segments comparing lateral disconnection stumps (ReTm) with junctional nodes. Note lower Ca and P in the stumps and a high Si *trend (nd = non-detectable).

Spectrum (mass %)							
	N	Si	Mg	P	Ca	Ca:P atom %	Ca:P mass%
Node 1	*nd*	*nd*	*nd*	8.7	16.2	1.56	1.88
Node 2	1.8	0.1	0.3	8.5	15.8	1.55	1.87
Stump 1	4.1	0.2	1.9	2.5	3.6	1.2	1.45
Stump 2	3.6	1.4*	0.3	2.8	4.6	1.36	1.64
Stump 3	3.6	1.4*	0.3	2.9	4.7	1.36	1.64

The new evidence now presented above from an osteopenic rodent model confirms the presence of sculptured bone fragments of variable size and with a topography closely defined by the number of their ReTm. Not only does FS morphology mirror their cancellous site of origin but also their vacated site adds to stacked forerunners contributing to ReTm hotspot domains. Under circumstances of metabolic or biomechanical stress these specific locations of sequential microdamage and altered force translation may function as predetermined zones of intrinsic weakness and potential deformation.

1) *Floating segments*, *microdamage and disconnection*.

The investigation derives from site-specific matrix microdamage characteristics (**Table 3**) instrumental in ReTm accumulation and structural instability.

The catabolic production of floating segments crosses species boundaries with local susceptibility being influenced by altered collagen (including withdrawal of Sharpey's fibre arrays), glycans or mineral content, the latter being especially variable due to its essential metabolic mobility, whether in response to the demands of multiparity or of aging. A precedent analysis by Shahtaheri *et al.* [8] had concerned the ex-breeder rat model in terms of its 2-dimensional histomorphometry by trabecular automated analysis (TAS); this had indicated a regional reduction in the connectivity index (as node: terminus ratio) together with a forty percent loss of struts (*c.f.* virgin controls). The subsequent 3-dimensional evaluation of trabecular disconnection in aging women went on to pinpoint ReTm cross-strut concentration within predestined hotspots of tensile weakness [5]. Within these domains can be traced a common sequential microdamage stress trajectory across polarised networks of transverse and vertical struts (**Figure 6**) consistent with the biomechanical maxim that acute tensile destabilisation of the former chronically undermines the compression resistance of the latter (*i.e.*, doubling the distance between cross-struts diminishes cancellous bone strength fourfold).

2) *Floating segments*, *microdamage*, *particle slip and crystal fracture.*

Microdamage is influenced by the fundamental nature of its bone matrix mineral. The reduced mineral density of individual ReTm stumps seems accountable by the release from inorganic compression and deformity of their composite populations of calcified microspheres (about 1 μm diameter; typically smaller in osteoporosis, 0.5 - 0.7 μm; larger in osteoarthritis, 0.5 - 4.0 μm [10]). Calcified with phosphate and morphologically and immunologically transmutable [11], the particles constitute an inorganic phase that is more biodynamically variable than the usual descriptions of static sheets of uniform hydroxyapatite crystals would suggest [12]. In addition, and structurally integral to the calcified microspheres, are the noncollagenous proteins (bone sialoprotein, osteopontin, osteocalcin) and inorganic molecules (carbonate, pyrophosphate, fluoride, silicon) which affect mineral amorphous/crystalline proportions in the matrix; in this way the nature of the mineral influences either "microparticle slip" or "crystal fracture" [13] as potential

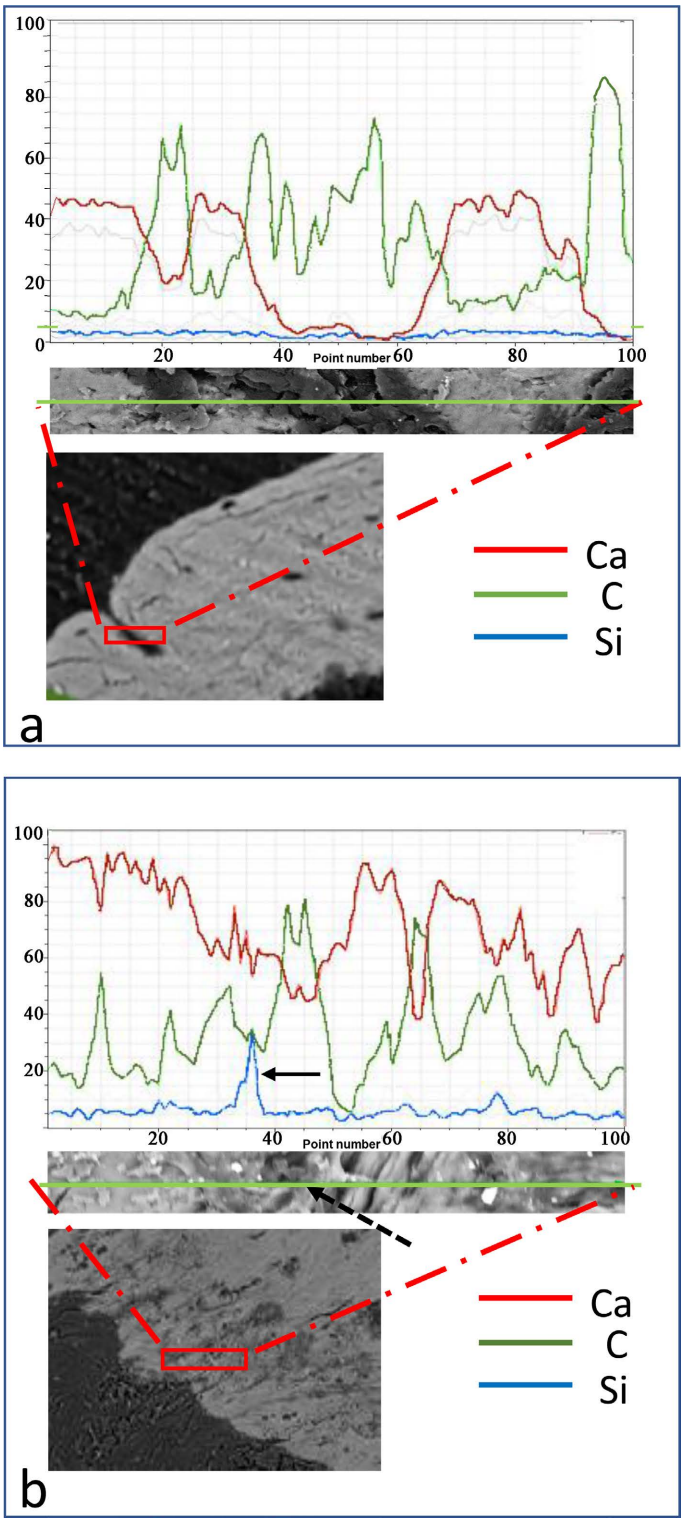

Figure 5. EDS line scans in relation to bone topography. (a) Line-scan across a point of trabecular severance similar to that seen in Figure 1(e), (b) Ca and P peaks in register with the topographic density profile related to fibrous insertions (dashed arrow) normally relatively uncalcified for functional stability and is associated with a strong Si peak(arrow). SEM. Plastic-embedded histological slices, 300 μm.

Table 3. **Microdamage morphology.**

1) Fractured trabecula.
2) Cortical and cancellous cracks.
3) Local leakiness to stains due to ultrastructural fissures.
4) Autoclastic matrix disaggregation into particles.
5) Cement lines as weak interfaces dispersing damaging forces elsewhere.

Table 4. **Microdamage and hydrogen bonds [13].**

Microparticle slip:
i) Mineral microspheres are both organically and aqueously encapsulated.
ii) At a crucial point of bone water content, hydrogen bonding between particles is powerful enough to support daily stresses (above/below this, bonds are weaker and particles more mobile).
iii) Cyclic stress disrupts hydrogen bonds causing particle slip (*i.e.* microdamage type I).
Crystal fracture:
i) Enamel mineral is exposed and crystalline.
ii) There is no water and little hydrogen bonding.
iii) When stressed, it displays crystal fracture along lattice planes (*i.e.* microdamage type II).
iv) There are circumstances when bone may behave like enamel by inherent fault or design (e.g. fluorosis).

underlying mechanisms of microdamage proliferation and structural failure (**Table 4**).

Previously reported as accommodating these twin facets of microdamage is a deformable ultrastructure of filamentous clusters composed of flexible strings of nanometre beads (5 nm) with a capacity for lateral filament fusion into rigid, autofluorescent, fenestrated plates [11, 12]. More generally, the micron-sized objects combine into convoluted, bridged assemblies, which interlock skeins of matrix collagen fibres into place for maximum strength, allowing the availability of less structurally committed mineral for free ionic exchange [13, 14]. At the same time, indigenous to the particulate populations is a complex extracellular biochemistry that includes hydrolytic enzymes such as carbonic anhydrase and acid phosphatase; these constitute an acellular autoclastic arsenal of microdamage mediation [15] which may not only be proactive in the weakening of cross-struts prior to FS development, but also is separate from osteoclasis to which it is inversely related.

3) *Floating segments and microdamage restitution.*

Damaged vertical struts may be reconfigured and restored by callus intervention (**Table 5**), when dissociated bone fragments reassemble into composite new trabeculae identifiable by their underlying disorder in polarised light [13]. The incidence of callus nodules around individual fractured trabeculae was illustrated by Vernon-Roberts and Pirie [6] in lumbar vertebrae from 22 spines. Their results showed the concentration of callus nodules occurred in the upper and lower thirds of each vertebral body where they were predominantly associated with vertical trabeculae (*i.e.*, subject to compression forces) and were rarely seen in relation to horizontal ones (*i.e.*, subject to tensile forces).

In the latter case, damaged cross-struts sometimes regain interconnection by emergent bridging scaffolds of endosteal Sharpey's fibres as deeply penetrating, intraosseous arrays of normally uncalcified, collagen type III/VI fibres. Derived from the periosteum their presence protects critical domains of tendon/ligament anchorage from destabilising remodelling [16], thereby maintaining the *status quo* and paradoxically

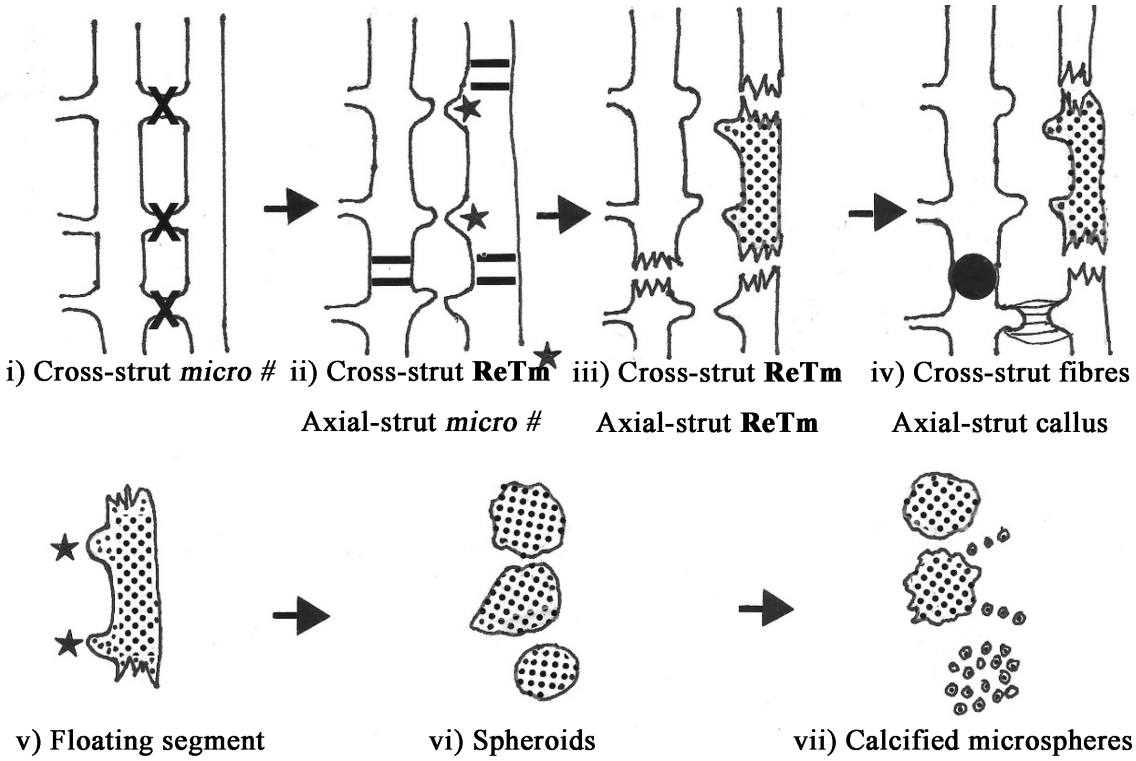

Figure 6. **Diagram summarising stages in sequential FS disconnection within ReTm hotspots. i) Serial tensile cross-strut microdamage (X) causes ii) stacked cross-strut severance ReTm* and axial compression overload (=), creating ii) axial deformation microcracks and ReTm disconnection which detach a floating sector (shaded). iv) Callus repair (black spot) confined to a vertical axial-strut may inhibit FS loosening elsewhere, while transverse bridging cross-strut fibres (striations) may also intervene. v) A typical FS (shaded area) composed of an axial-strut and stumps of serial lateral cross-struts. vi) Attrition reconfigures convoluted floating segments into bony spheroids, while further erosion vii) exposes constituent particulates calcified with the phosphate, which disseminate to the bloodstream inorganic elements with a biochemical payload of uncertain extraskeletal significance (e.g., osteocalcin hormone).**

Table 5. **Factors influencing repair potential.**

i) Microdamage is likely at a tolerable daily level and increases exponentially with age.
ii) Microcallus marks repair.
iii) Microcallus stiffens subchondral bone in the osteoarthritic femur and vertebral struts in the osteopenic spine.
iv) Repair may fail due to a decline in perception (via osteocytes?) or reaction (via remodelling).
v) Some areas are more at risk; immunohistochemically-defined matrix domains differ in macromolecular composition and also in the presence of Sharpey's fibres, influencing response to stimuli and remodelling.
vi) Fractured axial, compression-resistant trabeculae stimulate microcallus more readily than do cross-strut, tensile trabeculae.

exposing it to unchecked fatigue microdamage ([13, 15], *i.e.*, reminiscent of the low remodelling/high microdamage outcome of fluoride therapy). In particular, the immunohistochemical decline of these variably permeating and essentially uncalcified fibres has been shown to occur with age [17] and has been identified in

advance of oestrogen-related bone loss, when positive sites become negative and therefore no longer protected from remodelling [18]. Conversely, exercise stimulates their expansion [19]. In this way, attention to factors governing intrinsic hormonal status and extrinsic force translation via Sharpey's fibres may combine to control the future incidence and morphogenesis of floating bone segments.

4) *Floating segments and serially microdamaged cross-struts as potential "crumple zones".*

As vehicles of disconnection, floating segments seem to offer a comparative index of altered fracture predisposition in biomechanically contrasting skeletal pathologies, where the rate of cancellous disconnection is significantly increased. For example, the ReTm population is abnormally elevated both in low stress osteoporosis (OP) and in high stress osteoarthritis (OA), the distinction between the two being a matter of their differing ReTm distribution patterns [5]. In OP the ReTm are mainly sector-specific (*i.e.*, clustered within predictable hotspots) and transaxial (*i.e.*, located on tensile cross struts [5]). In OA, however, ReTm incidence is more random, apparently deflected by aberrant, extraneous forces and inadequate articular cartilage buffering. The contrasting disconnection patterns suggest that a cross-strut register of stacked ReTm equips OP (but not OA) with intrinsic microskeletal "crumple zone" constructs of controlled deformation * (**Figure 7**) releasing floating segments and stimulating the intervention of vertically polarised callus repair to soften the trajectory towards wedging or crush fracture. However, in OA in *extremis*, there sometimes occur subchondral, discrete, rounded bone marrow lesions (BML; approximately 15mm diameter). These pathological assemblies of broken trabeculae within a rounded perimeter have a cyclic capacity for restitution that resembles the discretely localised insult of bone biopsy trephine ablation followed by recovery [20]). As particularly capricious microcosms of fragmentation and lysis BML may be regarded as self-contained "crumple zones" spatially configured in reaction to the displaced excesses of OA kinetics.

"Crumple zone theory" is not entirely new. It has a gross anatomical history recounted by Cai *et al.* [21; citing Le Fort, 1901] to explain the structural complexity of the paranasal sinuses and arrives at the conclusion that, among other varied functions, the frontal sinus is likely to absorb and distribute energy consistent with its vital role as a crumple zone protecting the orbit and brain from craniofacial trauma.

5) *Floating, segments and "crumple zones", some limitations and prospects.*

Floating segments may be dismissed as preparation artefacts [14], although their frequently rounded outlines, as well as occasional breaks, suggest otherwise. In defining their morphogenesis without the benefit of immunohistochemical consolidation [22, 23] there is the risk of a dynamic overinterpretation of static images. Nevertheless, it has been commented by others that the proposed floating segment prospect "characterises a combination of high values of sensitivity, correctness, reproducibility, layer-by-layer resolution

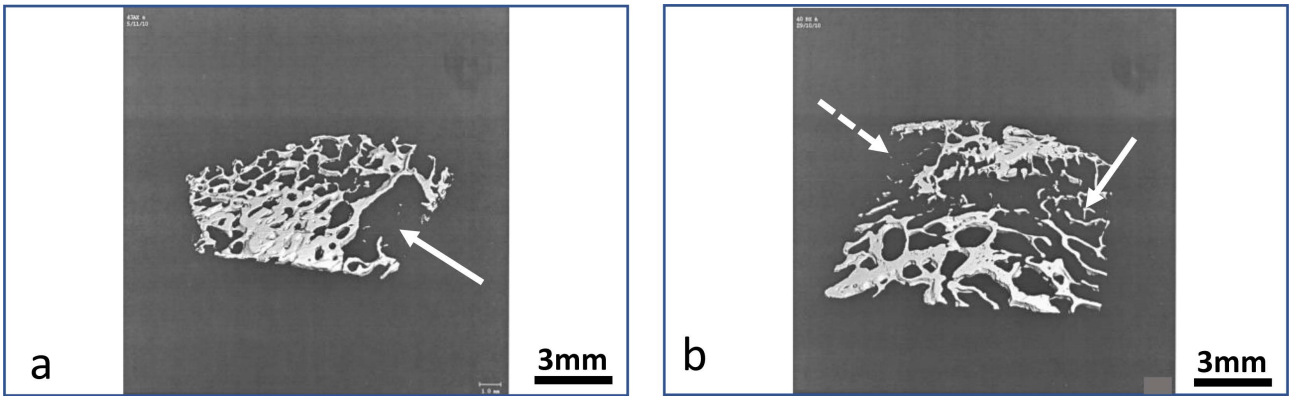

Figure 7. Postulated "crumple zones" (arrowed) in microCT images of electronic sections from elderly subjects, one (a) showing an almost vacuous, discrete "crumple zone" in an otherwise relatively dense spongiosa (BV/TV 25%); the other (b) in a less dense spongiosa (BV/TV 18%) showing two apparently adjoined and more diffuse "crumple zones", one (dotted arrow) containing fewer floating segments than the other (solid arrow). Preparation courtesy of Dr Pip Garner.

Table 6. Summary of evidence-based trabecular disconnection characteristics now directing the proposed road from "hotspots" to "crumple zones" via "floating bone segments", and apparently influenced by permeating intraosseous Sharpey's fibre arrays.

1) *Established histomorphometry methods showed no distinction between fracture and nonfracture groups with the same bone volume.* [3]

BUT a novel bespoke histology method [1] *identified trabecular disconnection as 4 × more prevalent in fracture than nonfracture groups with the same bone volume.* [3]

2) *Trabecular disconnection relates primarily to tensile cross-strut microdamage* [6], *which unlike vertical strut damage rarely stimulates callus* [13]. *In embryogenesis, de novo cross-struts derive from a scaffold of Sharpey fibres while vertical struts derive from a cartilage model* [27].

3) *Trabecular disconnection is reduced by bisphosphonate drugs.* [24]

4) *Trabecular disconnection is age-related and its mapping pinpoints "hotspot" clusters of weakness that are sex- and sector-specific.* [5]

5) *Trabecular disconnection in predictable "hotspots" may release "floating bone segments" and function as "crumple zones" of controlled deformation.* [5]

6) *Trabecular disconnection "hotspots" are a biomechanical frontier, the gatekeeper to which may be periosteal Sharpey's fibres (collagen Type III/VI); these regulate cross-strut microdamage, their uncalcified intraosseous presence protecting from osteoclasis.* [16]

BUT periosteal Sharpey's fibre arrays calcify and fragment with age; they expand with exercise and retract in oestrogen-deficiency; they atrophy prior to bone loss in osteoporosis and become hypertrophic in osteoarthritis. [17-19]

[**Footnote*: "*Crumple zone*" *definition. Structural safety zones used in vehicles to increase the time over which a change in velocity occurs from collision impact by controlled deformation dissipating kinetic energy into controlled deformation.*]

and the speed of layer-by-layer analysis". It follows that their varying numbers released from predestined disconnection hotspots (e.g., the distal inferior and proximal superior femoral head in women) may provide a novel morphometric of tensile force impact with potential relevance for i) mathematical modelling, ii) damaging extraneous physical activities, iii) optimal implantation sites for clinical factors and fillers and iv) as a potential factor in therapeutic fracture inhibition (for example, bisphosphonates apparently inhibit ReTm trabecular disconnection [24]). Observations above relate primarily to the female skeleton, where ReTm numbers were previously found to be typically denser and more clustered in *tensile* sectors (e.g., the anterior superior vertebral body in women) than seems to be the case in males (e.g., the *compression* sectors of the central vertebral endplates in men [25, 26]). This suggests that tensile transduction is a prime instigator of weakness at vulnerable locations in women, while the major factor in men is compression force.

5. CONCLUSION

In conclusion, a microskeletal feature of regional vulnerability that is independent of the bone volume is suggested for future consideration (**Table 6**). The morphogenesis of floating bone segments seems commensurate with concerted mechanical (direct/acute) or metabolic (indirect/chronic) microdamage proliferation taking place primarily within predetermined ReTm hotspot domains. Here serially severed

tensile cross-struts cause secondary vertical-strut compression overload, creating disconnections stacked into substructural "crumple zones" of deformation, where differential callus may occasionally intervene as a buffer to energy dissipation. After separation, the floating segments may persist within the marrow space as redundant objects, (where their numbers are an index of potential fracture predisposition) or regress into spheroids of uncertain bioactivity and vascular dispersion. Like perimeter ice shelves collapsing into the ocean, they may mark a more radical event, the scale of which remains to be determined.

ACKNOWLEDGMENTS

JEA and PAS are grateful to Action Medical Research and the HSA Charitable Trust for early sequential project support in developing the concept of cancellous disconnection hotspots as a defining factor in fragility fractures of the spine and hip.

CONFLICTS OF INTEREST

The authors declare no conflicts of interest regarding the publication of this paper.

REFERENCES

1. Shore, P.A., Shore, R.C. and Aaron, J.E. (2000) A Three-Dimensional Histological Method for Direct Determination of the Number of Trabecular Termini in Cancellous Bone. *Biotechnic & Histochemistry*, **75**, 183-192. https://doi.org/10.3109/10520290009066499
2. Hordon, L.D., Raisi, M., Aaron, J.E., Paxton, S.K., Beneton, M. and Kanis, J.A. (2000) Trabecular Architecture in Women and Men of Similar Bone Mass with and without Vertebral Fracture: I. Two-Dimensional Histology. *Bone*, **27**, 271-276. https://doi.org/10.1016/S8756-3282(00)00329-X
3. Aaron, J.E., Shore, P.A., Shore, R.C., Beneton, M. and Kanis, J.A. (2000) Trabecular Architecture in Women and Men of Similar Bone Mass with and without Vertebral Fracture: II. Three-Dimensional Histology. *Bone*, **27**, 277-282. https://doi.org/10.1016/S8756-3282(00)00328-8
4. Aaron, J.E., Makins, N.B. and Sagreiya, K. (1987) The Microanatomy of Trabecular Bone Loss in Normal Aging Men and Women. *Clinical Orthopaedics and Related Research*, **215**, 260-271. https://doi.org/10.1097/00003086-198702000-00038
5. Aaron, J.E., Shore, P.A., Itoda, M., Morrison, R.J.M., Hartopp, A., Hensor, E.M.A. and Hordon, L.D. (2015) Mapping Trabecular Disconnection "Hotspots" in Aged Human Spine and Hip. *Bone*, **78**, 71-80. https://doi.org/10.1016/j.bone.2015.04.009
6. Vernon-Roberts, B. and Pirie, C.J. (1973) Healing Trabecular Microfractures in the Bodies of Lumbar Vertebrae. *Annals of the Rheumatic Diseases*, **32**, 406-412. https://doi.org/10.1136/ard.32.5.406
7. Shahtaheri, S.M., Aaron, J.E., Johnson, D.R. and Purdie, D.W. (1999) Changes in Trabecular Bone Architecture in Women during Pregnancy. *BJOG: An International Journal of Obstetrics & Gynaecology*, **106**, 432-38. https://doi.org/10.1111/j.1471-0528.1999.tb08296.x
8. Shahtaheri, S.M., Aaron, J.E., Johnson, D.R. and Paxton, S.K. (1999) The Impact of Mammalian Reproduction on Cancellous Bone Architecture. *Journal of Anatomy*, **194**, 407-421. https://doi.org/10.1046/j.1469-7580.1999.19430407.x
9. Aaron, J.E. and Shore, P.A. (2004) Histomorphometry. In: Langton, C.M. and Njeh, C.F., Eds., *The Physical Measurement of Bone*, Institute of Physics Publishing, Bristol, Philadelphia, 185-224. (Citing Odgaard, A., Anderson, K., Melsen, F. and Gunderson, H.J. (1990) J Microsc, 159, 335-342. Also: Odgaard, A., Anderson, K., Ullerup, R., Frich, L.H. and Melsen, F. (1994) Bone, 15, 202-203)
10. Linton, K.M., Hordon, L.D., Shore, R.C. and Aaron, J.E. (2014) Bone Mineral "Quality": Differing Characteristics of Calcified Microsphere Populations at the Osteoporotic and Osteoarthritic Femoral Articulation Front. *Journal of Biomedical Science and Engineering*, **7**, 739-755. https://doi.org/10.4236/jbise.2014.79073
11. Carter, D.H., Scully, A.J., Heaton, D.A., Young, M.P.J. and Aaron, J.E. (2002) Effect of Deproteination on Bone Mineral Morphology: Implications for Biomaterials and Ageing. *Bone*, **31**, 389-395. https://doi.org/10.1016/S8756-3282(02)00840-2
12. Aaron, J.E. (2016) Cellular Ubiquity of Calcified Microsphere: A Matter of Degree, Ancient History and the Golgi Body?

Journal of Biomedical Sciences, **5**, 1-5. (Also: Top 10 Contributions on Biomedical Sciences: 2nd Edition. Avid Science 2018; 2-14) https://doi.org/10.4172/2254-609X.100037

13. Aaron, J.E. (2003) Bone Turnover and Microdamage. *Advances Osteopor Fracture Management*, **2**, 102-110.
14. Aaron, J.E., Oliver, B., Clarke, N. and Carter, D.H. (1999) Calcified Microspheres as Biological Entities and Their Isolation from Bone. *The Histochemical Journal*, **31**, 455-470. https://doi.org/10.1023/A:1003707909842
15. Aaron, J.E. (1976) Autoclasis—A Mechanism of Bone Resorption and an Alternative Explanation for Osteoporosis. *Calcified Tissue Research*, **22**, 247-254. https://doi.org/10.1007/BF02064074
16. Aaron, J.E. (2012) Periosteal Sharpey'S Fibres: A Novel Bone Matrix Regulatory System? *Frontiers in Endocrinology*, **3**, Article 98. https://doi.org/10.3389/fendo.2012.00098
17. Al-Qtaitat, A., Shore, R.C. and Aaron, J.E. (2010) Structural Changes in the Ageing Periosteum Using Collagen III Immunostaining and Chromium Labelling as Indicators. *Journal of Musculoskeletal and Neuronal Interactions*, **10**, 112-123.
18. Luther, F., Saino, H., Carter, D.H. and Aaron, J.E. (2003) Evidence for an Extensive Collagen Type III/VI Proximal Domain in the Rat Femur: I. Diminution with Ovariectomy. *Bone*, **32**, 652-659. https://doi.org/10.1016/S8756-3282(03)00094-2
19. Saino, H., Luther, F., Carter, D.H., Natali, A.J., Turner, D.L., Shahtaheri, S.M. and Aaron, J.E. (2003) Evidence for an Extensive Collagen Type III Proximal Domain in the Rat Femur: II. Expansion with Exercise. *Bone*, **32**, 660-668. https://doi.org/10.1016/S8756-3282(03)00095-4
20. Aaron, J.E. and Skerry, T.M. (1994) Intramembranous Trabecular Generation in Normal Bone. *Bone and Mineral*, **25**, 211-230. https://doi.org/10.1016/S0169-6009(08)80240-1
21. Cai, S.C., Mossop, C., Diaconu, S.C., Hersch, D.S., AlFadi, S., Rasko, Y.M., Christy, M.R., Grant, M.P. and Nam, A.J. (2017) The "Crumple Zone" Hypothesis: Association of Frontal Sinus Volume and Cerebral Injury after Craniofacial Trauma. *Journal of Cranio-Maxillofacial Surgery*, **45**, 1094-1098. https://doi.org/10.1016/j.jcms.2017.04.005
22. Chin, M. and Aaron, J.E. (2019) Sharpey Fibre Biologic Model for Bone Formation. In: Jensen, O.T., Ed., *The Sinus Bone Graft*, Quintessence Publishing, Berlin, London, 213-225.
23. Carter, D.H., Sloan, P. and Aaron, J.E. (1991) Immunolocalization of Collagen Types I and III, Tenascin and Fibronectin in Intramembranous Bone. *Journal of Histochemistry & Cytochemistry*, **39**, 599-606. https://doi.org/10.1177/39.5.1707904
24. Hordon, L.D., Itoda, M., Shore, P.A., Shore, R.C., Heald, M., Brown, M., Kanis, J.A., Rodan, G.A. and Aaron, J.E. (2006) Preservation of Thoracic Spine Microarchitecture by Alendronate: Comparison of Histology and MicroCT. *Bone*, **38**, 444-449. https://doi.org/10.1016/j.bone.2005.09.020
25. Garner, P., Wilcox, R. and Aaron, J. (2014) Computer-Assisted Method for the Spatial 3D Mapping of Trabecular Disconnections in the Spine. *Orthopaedic Proceedings*, **96-B**, 52.
26. Garner, P.A. (2012) Bone Ageing and Structural Disconnection. University of Leeds, Leeds.
27. Carter, D.H., Sloan, P. and Aaron, J.E. (1992) Trabecular Generation de Novo. A Morphological and Immunohistochemical Study of Primary Ossification in the Human Femoral Anlagen. *Anatomy and Embryology*, **186**, 229-240. https://doi.org/10.1007/BF00174144